

# Microcalorimetric study of the self-discharge of the NiOOH/Ni(OH)<sub>2</sub> electrode in a hydrogen environment

Z. MAO\*, A. VISINTIN, S. SRINIVASAN†, A. J. APPLEBY

*Center for Electrochemical Systems and Hydrogen Research, Texas A&M University, College Station, Texas 77843-3402, USA*

H. S. LIM

*Hughes Aircraft Company, Electron Dynamics Division, Torrance, California 90509-2999, USA*

Received 1 March 1991; revised 2 August 1991

A microcalorimetric method has been used to investigate the self-discharge behaviour of nickel oxyhydroxide electrodes in a pressurized gaseous hydrogen environment. It was found that the heat generation rate is proportional to hydrogen pressure, and is significantly dependent on the immersion state of the electrode in the electrolyte. Hence, diffusion of dissolved hydrogen gas towards or within the electrode controls, at least partially, the self-discharge rate. However, the heat generation decreases exponentially with time, indicating that self-discharge is also proportional to the amount of the charged active material available for the reaction. The presence of Mg, Co and Cd oxides or hydroxides appears to inhibit self-discharge. It was found that direct chemical reaction between dissolved hydrogen and the active material dominates, while in addition, electrochemical oxidation of hydrogen coupled with electrochemical reduction of the active material might also occur at a much smaller rate than the direct reaction.

## 1. Introduction

The self-discharge rate of a nickel-hydrogen battery is relatively high when compared with other types of secondary batteries. A typical nickel-hydrogen cell may lose one half of its charge in ten to fifteen days when it is stored at room temperature. The high self-discharge rate limits some applications of the cell. However, the mechanism of the self-discharge is not well understood. Thermodynamic data indicate that hydrogen can be oxidized by the active material (NiOOH) of the nickel electrode in a nickel-hydrogen cell. In the state-of-the-art nickel-hydrogen battery, hydrogen is accessible to the active NiOOH either directly in the gaseous state or through a thin layer of KOH electrolyte in the dissolved state. A widely speculated self-discharge mechanism is that hydrogen is electrochemically oxidized at the sintered nickel substrate as the rate limiting step while this oxidation is matched by reduction of NiOOH. But recent studies [1-3] could not confirm such a mechanism of self-discharge and indicate that a direct chemical reaction between hydrogen and NiOOH is a likely mechanism. It is important to understand the mechanism of self-discharge to control its rate in the nickel-hydrogen battery.

Microcalorimetry has been used for studies of self-discharge rate of lithium and other batteries [4, 5]. The microcalorimetric method is particularly useful because of its high sensitivity. It allows direct monitoring of

the heat flux, providing an advantageous means of in-situ characterization of the self-discharge rate. A previous study, using nickel oxide powder fully immersed in the electrolyte, indicated that the predominant mechanism of self-discharge is the direct chemical reaction between hydrogen and nickel oxyhydroxide [1]. The dependence of the self-discharge rate of nickel oxide/hydroxide electrodes on hydrogen pressures, the sintered nickel substrate, immersion state of the electrode, and the presence of metal additives, among other parameters, is presented in this work.

## 2. Experimental details

### 2.1. Electrode preparation

The test samples used in the experiments were: (i) nickel oxyhydroxide electrodes, which are used in aerospace Ni-H<sub>2</sub> flight cells [6] and contain about 10% cobalt in the active material; (ii) identical electrodes with additional hydroxide impregnation using an electrochemical method in 0.6 M Cd(NO<sub>3</sub>)<sub>2</sub> solution; or (iii) electrodes prepared in our laboratory, using a modified electrochemical impregnation of a dry powder type sintered nickel plaques. The sintered nickel plaques (porosity about 82%, thickness 0.75 mm), were cut into 2.5 cm squares, which were ultrasonically cleaned in deionized water, and activated for about 20 s in a dilute nitric acid solution.

\* Present address: Department of Chemical Engineering, Texas A&M University, College Station, Texas 77843-3122.

† Corresponding author.

They were then introduced into a rectangular impregnation cell designed for location of three electrodes. The deposition solution contained 2M total metal nitrate solution in 50:50 volume % ethanol-water. The nitrate was 2 M pure nickel nitrate, or 1.8 M nickel and 0.2 M metal additive nitrate. The latter included Co, Cd, Mg or Zn. The plaques were cathodically impregnated at a constant current density of  $93 \text{ mA cm}^{-2}$  for 2 h at about  $80^\circ \text{C}$ , i.e., the boiling point of the solution. The resulting nickel hydroxide electrodes were activated and stabilized by fully charging and discharging in 20 wt % KOH solution for four cycles at a current density of  $118 \text{ mA cm}^{-2}$ . The nominal electrode capacity was determined from the discharge potential vs time plot at  $7.75 \text{ mA cm}^{-2}$ , corresponding approximately to the C/3-C/4 rate. After being fully charged, the electrodes were cut into smaller pieces of the desired size, and immediately transferred into the microcalorimeter cell for the experiments.

## 2.2. Microcalorimeter

A commercial microcalorimeter (Hart Scientific Inc., Model 5024) was used. This is a twin chamber heat conduction calorimeter, coupled with a computer for data acquisition. The instrument measures heat flux via the Seebeck effect. The multiple thermoelectric junctions are mounted between the measuring chamber and a heat sink, the temperature of which is maintained constant at a desired value. The electrical response of the junctions is proportional to the temperature difference between the measuring cell and the heat sink. Thus by calibration using a standard resistor, the heat flux may be determined. The instrument has very low noise and excellent baseline stability and reproducibility, which are within  $1 \mu\text{W}$ . For calibration of the microcalorimeter, a standard  $1000 \Omega$  resistor was placed in the sample cell. Heat fluxes, equal to the input electrical power, were calculated from the voltage across this resistor by accurately passing desired currents produced by a Solartron 1286 Electrochemical Interface.

## 2.3. Measurement of heat generation rates

A small cylindrical cell was fabricated from a solid nickel bar for the microcalorimetric experiments. The cell was similar to the one used previously [1]; it had an internal volume of 5 ml and was connected to a stainless steel tube of 1/16 inch (about 1.6 mm) external diameter. Electrodes, prepared as described above, were cut into 1 cm by 0.5 cm strips. Three such strips and 0.8 ml of 31 wt % KOH solution were introduced into the cell the electrodes were in a fully immersed state. Hydrogen was then passed through the cell to flush out air; the cell was sealed, and the hydrogen pressure was raised to the desired value. The heat flux at  $25^\circ \text{C}$  was then determined as a function of time at different pressures.

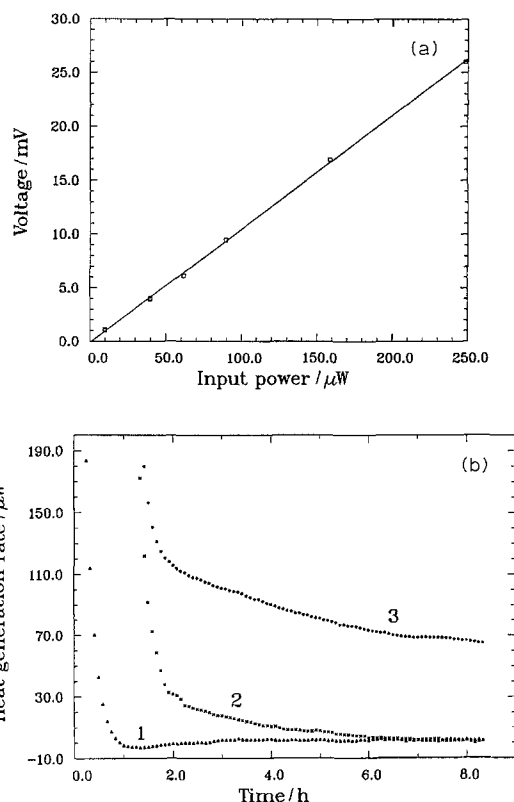


Fig. 1. (a) Calibration curve for the microcalorimeter and (b) typical calorimetric curves at a pressure of 700 p.s.i. for three cases: (1) sintered nickel substrate in hydrogen environment; (2) nickel oxyhydroxide electrode in argon environment; (3) nickel oxyhydroxide electrode in hydrogen environment. The electrodes for 2 and 3 were prepared from 1.8 M  $\text{Ni}(\text{NO}_3)_2$  and 0.2 M  $\text{Zn}(\text{NO}_3)_2$  solution, and the capacity of the electrodes was  $16 \text{ mAh cm}^{-2}$ .

## 3. Results and discussion

### 3.1. Calorimeter calibration

Figure 1a shows the calibration curve of the microcalorimeter. It shows that both microcalorimeter sensitivity and linearity of the output sensor voltage-input electrical power relationship are excellent. Figure 1b shows typical heat flux measurements for three different cases, and also demonstrates that it requires about 2 h for the microcalorimeter to stabilize after the sample cell was introduced into the chamber. Thus, only after this time are the results meaningful. They show that the active NiOOH electrode, in a hydrogen environment, released a considerable amount of heat, whereas the same material under argon, or the nickel sinter alone under hydrogen, showed negligible reaction rates.

### 3.2. Effect of hydrogen pressure

Figure 2a shows plots of heat generation rates as a function of hydrogen pressure for the electrodes with and without additives. These were linear for all the electrodes, indicating that the reaction order with respect to hydrogen pressure is unity. A possible explanation is that the reaction rate may be controlled by the diffusion of dissolved hydrogen towards (or within) the electrode. Other work has also shown that

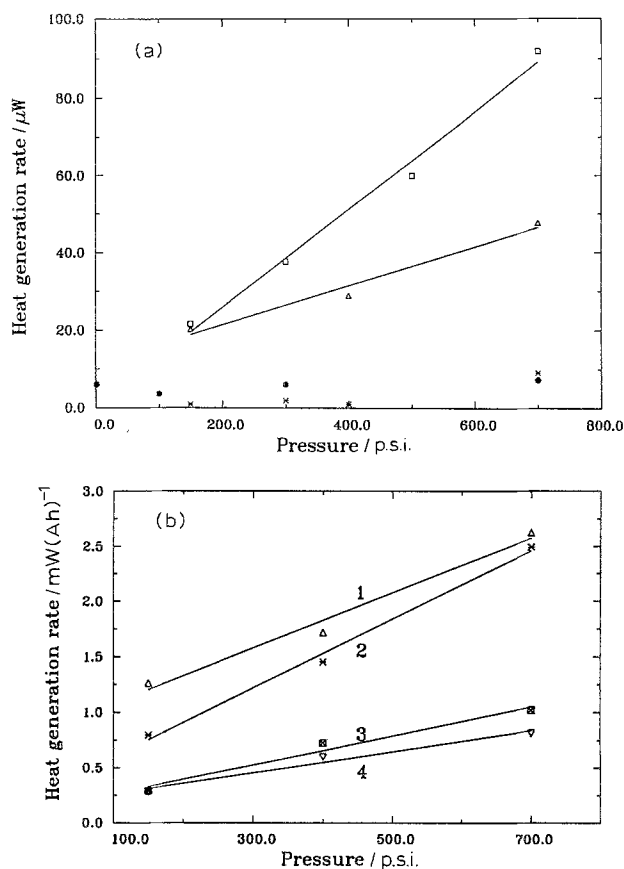


Fig. 2. Heat generation rate as a function of hydrogen pressure. Data were taken 8 h after the experiment was started. (a) Electrodes provided by Hughes Aircraft Company, (□) the electrodes also contain Co; (Δ) the electrodes also contains both Co and Cd, (\*) same electrodes as (◇) but in argon environment, (●) sintered nickel substrate in hydrogen environment. (b) The electrodes prepared in this laboratory. (Δ) the electrode contains Zn, (\*) the electrode contains Cd, (□) the electrode contains Co, (▽) the electrode contains Mg.

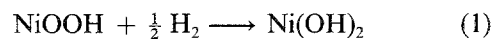
the pressure in Ni-H<sub>2</sub> batteries decreases exponentially with time, which is characteristic of a first order reaction [7]. However, it has also been reported that the interfacial reaction controls battery self-discharge [8]. In contrast to the present set of experiments, electrodes used in the above mentioned work were not fully immersed in the electrolyte.

Since the electrodes in the present experiments were immersed in the electrolyte, diffusion of dissolved hydrogen may partially control reaction rate; a simple calculation is given below to estimate the magnitude of the heat flux under such conditions. The solubility of hydrogen gas in 31 wt % KOH electrolyte is  $5.505 \times 10^{-8} \text{ mol cm}^{-3} \text{ atm}^{-1}$  [9], and based on the theoretical equation in [10], its diffusion coefficient is approximately  $1.53 \times 10^{-5} \text{ cm}^2 \text{ s}^{-1}$ . Assuming that Henry's law is still valid at high pressures and that the dissolved hydrogen diffuses through an electrolyte layer of average thickness 0.2 cm, the diffusion rate at a hydrogen pressure of 49 atm ( $\sim 700$  p.s.i. or  $\sim 5 \times 10^6$  Pa) may be estimated as:

$$r_h = Dc_{\text{H}_2}/\delta = 2.10 \times 10^{-10} \text{ mol cm}^{-2} \text{ s}^{-1}$$

where  $D$  is the diffusion coefficient of dissolved hydrogen,  $c_{\text{H}_2}$  is the concentration of dissolved hydrogen at the given hydrogen pressure, and  $\delta$  is the diffusion

layer thickness. Expressing this diffusion rate as a reaction rate between hydrogen and NiOOH according to the overall reaction:



the heat generation rate is estimated to be  $59 \mu\text{W cm}^{-2}$ , based on an enthalpy change of  $-144.85 \text{ kJ mol}^{-1}$  for Reaction (1). This heat generation rate is of the same order of magnitude as those measured. Therefore, the diffusion of dissolved hydrogen may be at least partially controlling under these experimental conditions. However, it should be noted that the magnitudes and slopes of the heat flux as a function of time differ from one experiment to another, and that the composition of the electrode active material also affects self-discharge rate. The diffusion of dissolved hydrogen towards the electrodes cannot be the sole rate-controlling process; otherwise, the heat flux would be expected to be the same for all these similarly immersed electrodes. The  $\text{mW(Ah)}^{-1}$  used in Fig. 2b allow a comparison of the effects of metal additives (see below).

Heat generation rates for the electrodes in an argon environment are also shown in Fig. 2a. The rates are very small and are independent of argon pressure. There is therefore no question that the observed heat generation rate represents the reaction between dissolved hydrogen in the flooded electrolyte and nickel oxyhydroxide.

### 3.3. Effect of metal additives

If the rate of the self-discharge reaction is controlled by some surface processes, then it would depend on the intrinsic electrode surface properties. Modification of these properties by the use of metal additives, particularly those with high overpotentials for the hydrogen oxidation, may result in a slower self-discharge kinetics. To compare the differences between the effects of such additives, heat generation rates were determined for unit capacities of the electrode, as Fig 2b and 3 show. Among the additives studied, Mg has some beneficial effect on self-discharge. Electrodes containing both Cd and Co gave much lower heat fluxes than those containing Co alone. However, it should be borne in mind that because electrode morphology influences heat generation rate, and electrodes with the same morphology and material loading are difficult, if not impossible, to prepare from the solutions containing different metal additives, the effect of the additives on self-discharge may deviate somewhat from those shown in Figs 2b and 3 when all these factors are taken into account. Figure 4 indicates that heat generation rate or self-discharge increases linearly with initial capacity. Both the total amount of active material and the effect of surface roughness, which is higher for high-capacity electrodes, contribute to this result.

### 3.4. Effect of time

As Fig. 3 shows, the heat generation rate decreases

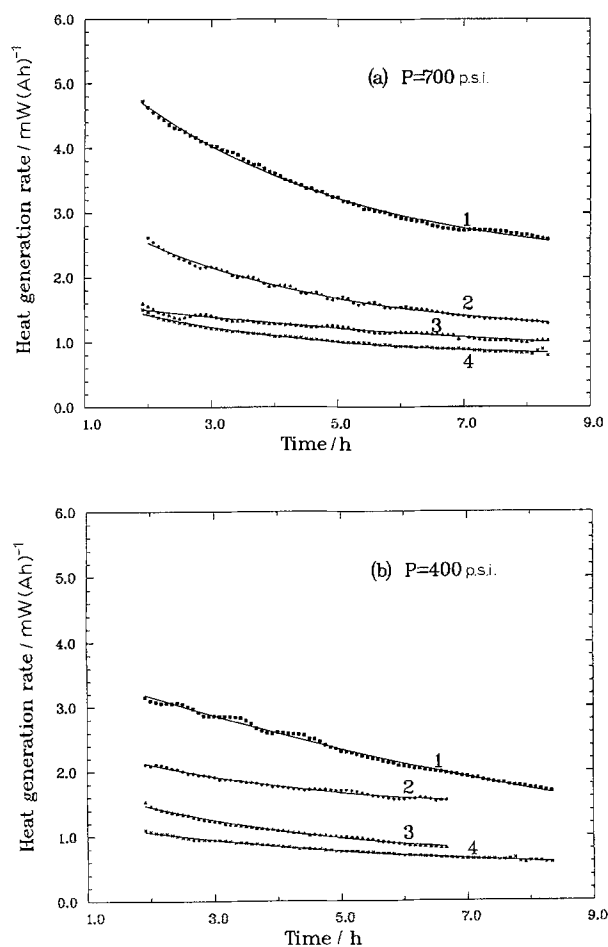


Fig. 3. (a) Calorimetric curves at 700 p.s.i., (b) at 400 p.s.i. Electrodes prepared in this laboratory. (1) The electrode contains Zn, (2) the electrode contains Cd, (3) the electrode contains Co, and (4) the electrode contains Mg.

gradually with time at constant hydrogen pressure. This may reflect the change of the amount of active material in the electrode as self-discharge proceeds. If the diffusion of dissolved hydrogen does not affect the self-discharge, and the solid phase reaction in the electrode namely (i.e., the mixing reaction between  $\text{NiOOH}$  and  $\text{Ni}(\text{OH})_2$  via proton diffusion) is infinitely fast compared to the self-discharge rate [11, 12], the

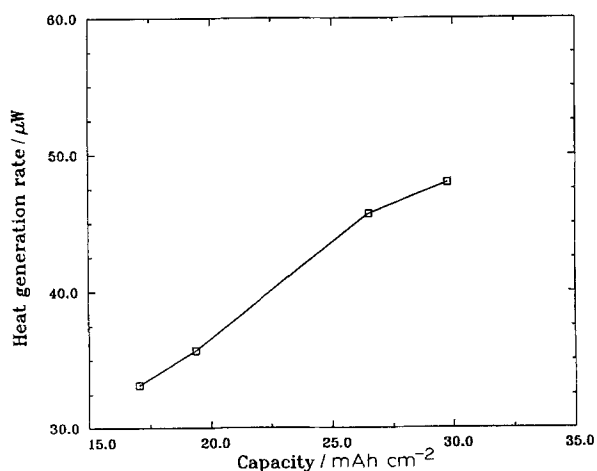


Fig. 4. The heat generation rate as a function of initial electrode capacity for the electrode with no additives at a hydrogen pressure of 700 p.s.i. Data were taken after 8 h.

self-discharge can be treated as a homogeneous chemical reaction, the rate of which may generally be expressed by the equation

$$r = kC_{\text{H}_2}^p C^q \quad (2)$$

where  $p$  and  $q$  are the reaction orders with respect to dissolved hydrogen ( $C_{\text{H}_2}$ ) and to the remaining amount of nickel oxyhydroxide (i.e., the capacity of the electrode,  $C$ ), respectively. Since the reaction rate is measured in terms of the heat generation rate as a function of time, at constant hydrogen pressure, the above equation can be rearranged as

$$r = KC_0 \exp(-Kt) \quad \text{for } q = 1 \quad (3)$$

$$r = K[C_0^{1-q} - (1-q)Kt]^{1-q} \quad \text{for } q \neq 1 \quad (4)$$

where  $K = kC_{\text{H}_2}^p$ ,  $C_0$  represents the initial capacity of the electrode, and  $t$  is the time. These equations were obtained by first integrating Equation 2 and then taking the derivative of  $C$  with respect to  $t$  to obtain the expression for  $r$  as a function of  $t$ . Figure 3 shows the theoretical plots and experimental calorimetric data of heat generation rates as a function of time on different electrodes at two hydrogen pressures. The symbols are experimental points, and the continuous curves fit equations of the form

$$r = a + b \exp(ct) \quad (5)$$

where  $r$  is the heat generation rate, and  $a$ ,  $b$  and  $c$  are constants. It was attempted to fit the experimental data to Equations 3 or 4, but the agreement was not as good as that using Equation 5 for either  $q = 1$  or for  $q \neq 1$ .

The less precise fit, i.e. using Equations 3 or 4 rather than Equation 5, may result from the fact that the experimental time spans are relatively short and that self-discharge is small in all the cases. It also suggests that the self-discharge reaction does not behave as a simple homogeneous chemical process. Mao and White [13] recently developed a mathematical model of the self-discharge of the Ni-H<sub>2</sub> battery, in which the diffusion of dissolved hydrogen through a thin layer of electrolyte covering the electrode is included and the solid phase reaction is assumed to be very fast. The prediction of the self-discharge rate as a function of time, under the conditions of the present experiments, is in agreement with the experimental results. It may be concluded that the heat generation rate is proportional to the amount of the active material which the dissolved hydrogen can access in what is presumably a single-phase oxide system with activity proportional to concentration. It was also observed that electrode morphology considerably affects the heat generation rate; for example, an electrode with a rough surface yields more heat than a smooth electrode. Since it is difficult to quantitatively assess the effect of electrode roughness and other parameters on heat generation rate, these aspects of self-discharge still remain to be further investigated.

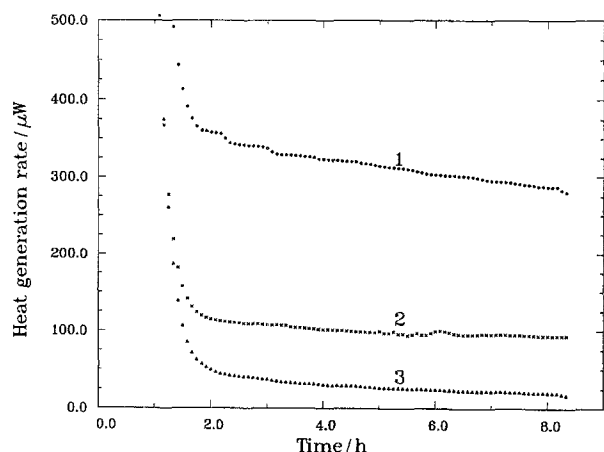


Fig. 5. Heat generation rate as a function of time for the electrodes in three immersion states with the electrolyte. Hydrogen pressure was 700 p.s.i. (1) "Barely" immersed; (2) partially immersed; (3) fully immersed. The electrode capacity was 24.8 mAh cm<sup>-2</sup>, with no additives, the electrolyte contained 4% wt LiOH and 27 wt% KOH.

### 3.5. Effect of immersion of electrodes

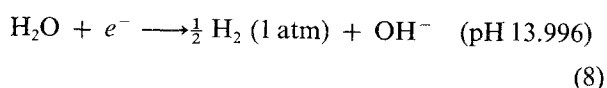
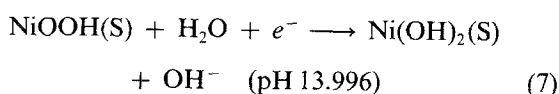
The linear relationship between heat generation rate and hydrogen pressure gives an indication that diffusion of dissolved hydrogen towards the electrode is one of the slow reaction steps. It would therefore be expected that partially immersed or electrolyte-starved electrodes should show a greater heat flux or self-discharge rate than flooded electrodes. Figure 5 shows typical microcalorimetric results for different electrode immersion states at a hydrogen pressure of 49 atm (~700 p.s.i. or ~5 × 10<sup>6</sup> Pa). The electrodes were either "fully immersed" (fully covered by electrolyte); "partially immersed" (with part of electrodes exposed to hydrogen gas), or "barely immersed". Figure 5 shows that a "barely immersed" electrode yielded a greater heat flux than one which was "fully immersed". Hence, diffusion of dissolved hydrogen through the bulk electrolyte considerably reduces self-discharge rate.

### 3.6. Estimation of self-discharge rate

The enthalpy change of Reaction 1 is needed in order to estimate the self discharge rates from the measured heat generation rates. Based on the method presented by Bratsh [14], the enthalpy change can be calculated using the equation

$$\Delta H = F(E_2^0 - E_1^0) - TF \left( \frac{\partial E_2^0}{\partial T} - \frac{\partial E_1^0}{\partial T} \right) \quad (6)$$

where  $E_1^0$  and  $E_2^0$  are the standard electrode potentials for half-cell Reactions 7 and 8, respectively:



for  $E_1^0 = 0.52 \text{ V}$ ,  $E_2^0 = -0.828 \text{ V}$ ,  $\partial E_1^0/\partial T =$

Table 1. Estimated capacity loss

Electrode†	Heat released/J(Ah) <sup>-1</sup> *	Capacity loss/%
NiMg700	72.47	1.3
NiCo 700	76.35	1.4
Ni 700	99.86	1.8
NiCd 700	111.11	2.1
NiZn 700	217.52	4.0
NiMg400	47.63	0.9
NiCo 400	62.20	1.1
NiZn 400	138.01	2.6

\* The heat generated for the first 24 h.

† The letters denote the elements the electrode contains, and the number represents hydrogen pressure in psig.

$-1.35 \times 10^{-3} \text{ VK}^{-1}$  and  $\partial E_2^0/\partial T = -0.836 \times 10^{-3} \text{ VK}^{-1}$  [14]. From these data,  $\Delta H$  is calculated to be  $-144.85 \text{ kJ mol}^{-1}$  or  $-5.404 \text{ kJ(Ah)}^{-1}$ . The capacity loss ( $L$ ) of an electrode within a certain period of time can be estimated from the equation:

$$L = \int_0^t \frac{rdt}{C_0 \Delta H} \times 100\% \quad (9)$$

$C_0$  is the total initial capacity of the electrode, and  $r$  is the heat generation rate. Tables 1 and 2 present the first day capacity losses of electrodes at different hydrogen pressures and in different states of immersion. The capacity loss for "fully immersed" electrodes at low hydrogen pressure is small. However, the capacity loss increases from less than 3% to more than 10% as one goes from "fully immersed" to "barely immersed" electrodes. The electrode containing magnesium hydroxide exhibited the smallest capacity loss. However, we should bear in mind that the percentage capacity loss for a large-capacity electrode will be less than that with a small capacity, even though the measured self-discharge rates are the same for the electrodes. The electrodes containing magnesium hydroxide had a higher capacity than the other electrodes even though they were prepared under the same conditions as those for the other electrodes.

### 3.7. Effect of substrate

Figure 6 shows the effect of the sintered nickel substrate on the heat generation rate. For these experiments, a small strip of nickel plaque was spot-welded to a NiOOH/Ni(OH)<sub>2</sub> electrode, and both were placed together in the cell. The heat generation rate increased, to a small extent, with increasing substrate area, indicating that hydrogen oxidation could occur

Table 2. Effect of immersion on heat generation rate\*

State of immersion	Heat released/J(Ah) <sup>-1</sup> †	Capacity loss/%
Bare	572.2	10.6
partial	172.9	3.2
Full	28.6	0.5

\* The solution consisted of 31 wt% alkaline metal hydroxide in which the ratio of Li/K was 1/7. The hydrogen pressure was 700 p.s.i.

† The heat generated for the first 24 h.

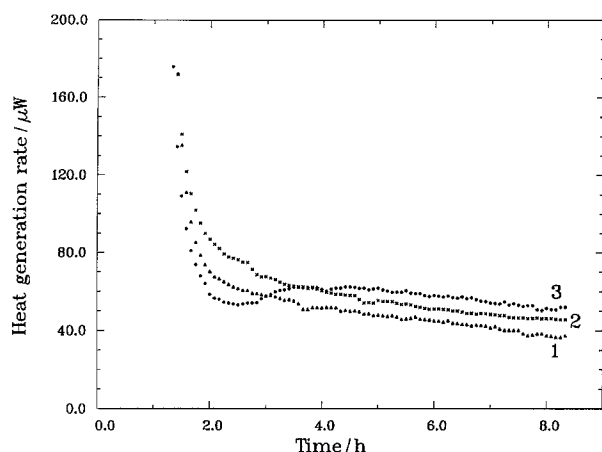


Fig. 6. Calorimetric curves at a hydrogen pressure of 700 p.s.i. for the electrodes coupled with a sintered nickel substrate of different size. The size of the electrodes was  $0.5 \times 2.4 \text{ cm}^2$  with a capacity of 39 mAh. (1) Substrate was not coupled, (2) the electrode was coupled with a substrate of the same size as the electrode, (3) the electrode was coupled with a substrate twice as large as the electrode.

separately on the nickel substrate in an electrochemical process, with simultaneous electrochemical reduction of nickel oxyhydroxide. While pure nickel is a good hydrogen oxidation electrocatalyst at low potentials (more negative than  $-0.75 \text{ V}$  against  $\text{Hg}/\text{HgO}$ ), at the potential of the nickel oxyhydroxide electrode (greater than  $0.2 \text{ V}$  against  $\text{Hg}/\text{HgO}$  electrode), its surface would be expected to consist of nickel hydroxide or nickel oxyhydroxide rather than metallic nickel. This oxidized nickel surface has a lower electrocatalytic activity for hydrogen oxidation than Pt or Au [15], which thus provides an explanation for the small increase of heat generation rate, even though the surface area for the electrochemical hydrogen oxidation reaction was by many times higher than on smooth metals.

#### 4. Conclusions

This investigation suggests the following conclusions: (i) the microcalorimetric method can be used to quantitatively study self-discharge behaviour of the Ni-H<sub>2</sub> battery; (ii) the heat generation rate, i.e., the self-discharge rate, is proportional to the amount of active material on the electrode surface; (iii) the heat generation rate is partially controlled by the diffusion of

dissolved hydrogen through the electrolyte layer covering the electrode; (iv) among the additives examined, (Co, Cd, Mg, Zn), it appears that Mg, or the combined presence of Co and Cd, has a beneficial effect for inhibition of hydrogen oxidation on the nickel oxyhydroxide electrode; and (v) a direct chemical reaction between nickel oxyhydroxide and dissolved hydrogen or an electrochemical oxidation of hydrogen at the NiOOH surface is the dominant mechanism of self-discharge, however, hydrogen oxidation can also take place separately on the sintered nickel substrate, but at a much smaller rate compared to that on the active material.

#### Acknowledgements

This work was sponsored by the Hughes Aircraft Company (Contract No. S8-529211-X13) and the NASA Center for Space Power at Texas A&M University (Contract No. NAGW-1194).

#### References

- [1] Y. Kim, A. Visintin, S. Srinivasan and A. J. Appleby, in 'Nickel Hydroxide Electrodes', (edited by D. A. Corrigan and A. H. Zimmerman), *The Electrochemical Society*, Pennington NJ, **90-4** (1990) p. 368.
- [2] A. Visintin, S. Srinivasan, A. J. Appleby and H. S. Lim, in press *J. Electrochem. Soc.*
- [3] H. S. Lim and D. B. Losee, 'Studies on Self-Discharge Mechanism of Ni-H<sub>2</sub> Cells', to be published.
- [4] L. D. Hansen and R. M. Hart, *J. Electrochem. Soc.* **125** (1978) 842.
- [5] L. D. Hansen and H. Frank, *ibid.* **134** (1987) 1.
- [6] D. F. Pickett *et al.*, Proceedings of the 15th Intersociety Energy Conversion Engineering Conference, Seattle WA (1980) p. 1918.
- [7] B. I. Tsenter and A. I. Sluzhenskii, *Z. Prikladnoi Khim.* **54** (1981) 2545.
- [8] G. Holleck, Proceedings of the 1977 Goddard Space Flight Battery Workshop, NASA Conference Publication (1977) p. 2041.
- [9] R. Battio and E. Wilhelm, 'IUPAC Solubility Data Series', (edited by C. L. Young), Pergamon Press, New York, **5/6** (1981) p. 33.
- [10] 'Chemical Engineering Handbook', 5th ed., (edited by R. H. Perry and C. H. Chilton), McGraw Hill, New York (1973), pp. 3-23.
- [11] G. W. D. Briggs and P. R. Snodin, *Electrochim. Acta* **27** (1982) 565.
- [12] D. M. MacArthur, *J. Electrochem. Soc.* **117** (1970) 729.
- [13] Z. Mao and R. E. White, *J. Electrochem. Soc.* **138** (1991) 3354.
- [14] S. G. Bratsh, *J. Phys. Chem. Data* **18** (1989) 1.
- [15] C. Zhang, R. E. White, J. Kim, A. J. Appleby and S. Srinivasan, in Y. Kim *et al.*, *op. cit.* [1], p. 356.